Future Changes in the Transitions of Monthly-to-Seasonal Precipitation Extremes over the Midwest in CMIP6 Models

Liang Chen (liangch@illinois.edu)
University of Illinois Urbana-Champaign
Trent W Ford
University of Illinois Urbana-Champaign

Research Article

Keywords: Precipitation Extremes, SPI, Midwest, CMIP6

Posted Date: April 14th, 2022

DOI: https://doi.org/10.21203/rs.3.rs-1527171/v1

Abstract

Precipitation extremes present significant risks to Midwest agriculture, water resources, and natural ecosystems. Recently, there is growing attention to the transitions of precipitation extremes, or shifts between heavy precipitation and drought, due to their profound environmental and socio-economic impacts. Changes in Midwest precipitation extremes and transitions between extremes over the past few decades have been documented; however, their future changes are still unknown. In this study, we estimate the projected changes in transitions of precipitation extremes in the Midwest based on 17 CMIP6 models. Two Standardized Precipitation Index (SPI) based metrics, intra-annual variability and transitions, are used to quantify the magnitude, duration, and frequency of variability and transitions between wet and dry extremes. Compared with the observation-based precipitation datasets, the multimodel ensemble median of CMIP6 can reasonably represent the spatial patterns of SPI extremes and transitions. Climate projections show significantly intensified wet extremes across the Midwest by the end of the century, with a greater increase over the northern Midwest and the Great Lakes region. The short-term SPI also shows intensified dry extremes over the western half of the Midwest. Consequently, there is a significant increase in the magnitude of intra-annual variability in most areas. Projections also suggest more frequent and rapid transitions between the wet and dry extremes, especially over the Great Lakes region and northern Midwest. Seasonally, more frequent transitions from a wet spring to a dry summer (or from a dry fall to a wet winter/spring) are projected to occur; and generally, the wet and dry conditions between the transitions are projected to be more intense compared to the historical period. Furthermore, the intensified precipitation extremes and accelerated transitions are greatly alleviated under a lower emission scenario, implying that future changes in hydroclimate extremes, and impacts thereof, in the Midwest are sensitive to climate change mitigation.

1. Introduction

The variations of precipitation extremes, such as heavy precipitation and drought, present major risks for natural and human systems. The US Midwest, one of the most agriculturally productive regions in the world (Berhane et al. 2020), can be heavily impacted by those extreme events, resulting in crop yield reduction, infrastructure damage, poor human and ecological health outcomes, and tremendous economic loss (Angel et al. 2018; Liu and Basso 2020). Historically, significant increasing trends in heavy precipitation have been observed in the Midwest (Janssen et al. 2014; Walsh et al. 2014). Historical changes in drought are more mixed, with some studies finding increasing drought frequency especially in the northern Midwest (Ficklin et al. 2015) and other studies reporting no change or largely decreasing drought risk in the Midwest (Mo and Lettenmaier 2018; Basso et al. 2021). Under a warming climate, precipitation extremes are expected to be more intense (Seneviratne et al. 2012), because the water holding capacity of the atmosphere increases with temperature according to the Clausius-Clapeyron scaling (Bador et al. 2018). Climate projections from state-of-the-art climate models (such as Coupled Model Intercomparison Project phase 6, CMIP6; North America Coordinated Regional Downscaling

Experiment, NA-CORDEX) have projected increased risks of floods and droughts in the future (Akinsanola et al. 2020; Chen and Ford 2021; Almazroui et al. 2021).

Although considerable attention has been given to the precipitation extremes by quantifying different precipitation indices independently (Akinsanola et al. 2020; Chen and Ford 2021), there is an increasing demand for a better understanding of the transitions between precipitation extremes, which may lead to more significant environmental and socio-economic impacts (Ford et al. 2021). Transitions between extremes, also described as “weather whiplash” (e.g., Cohen 2016), refers to the rapid evolution from one climate extreme to that of the opposite sign. Such transitions of precipitation extremes and their impacts have been documented in the Midwest. Christian et al. (2015) suggest that there is a considerable chance that a drought year is followed by a pluvial year in the US Great Plains. Loecke et al. (2013) attributed water quality problems in the Midwest to poor soil conditions and nutrient runoff due to the rapid transition drought in 2012 to pluvial in 2013. A more recent example was the widespread flooding across the Midwest in spring 2019, followed by rapid onset drought in the late summer 2019 over the southern Midwest, both of which resulted in reductions in crop yield (Yin et al. 2020). Our recent study explores Midwest precipitation extremes and transitions over the last 70 years, and finds that wet-to-dry transitions have largely increased in speed and frequency in many areas of the Midwest (Ford et al. 2021).

Despite the increased concerns about recent transitions of precipitation extremes and associated environmental and socio-economic impacts, little work has been done to estimate how the transitions will change in the future climate. Understanding future transitions is essential to Midwestern agriculture, especially considering the projected intensification of precipitation extremes. Therefore, the goal of the study is to investigate the projected changes in transitions of precipitation extremes in the Midwest using climate projections from CMIP6. We aim to answer two research questions: (1) Can CMIP6 models represent the regional precipitation extremes and transitions during the historical period? (2) How will the transitions change in different climate scenarios? The paper is organized as follows. A detailed description of data and methods is given in Section 2. Historical precipitation extreme transitions in CMIP6 are evaluated in section 3. The projected changes in the transitions and their seasonality are presented in section 4. Discussions and summaries are provided in section 5.

2. Datasets And Methodology

2.1 CMIP6 output

In this study, we use precipitation output from CMIP6 to quantify the present and future precipitation extremes. Two metrics developed in Ford et al. (2021) are applied to quantify the transition of precipitation extremes. We use simulated daily precipitation from 17 global climate models (GCMs) participating in CMIP6 to analyze the transitions of precipitation extremes. Previous studies have evaluated the performance of CMIP6 in simulating precipitation extremes in the US at continental or regional scales and suggest that multimodel median performs better overall than individual models (e.g., Akinsanola 2020; Srivastava et al. 2020). Also, there are studies assessing future changes in regional

precipitation extremes using CMIP6 (e.g., Tang et al. 2021; Xu et al. 2021). Those studies in model evaluation and extreme assessment have demonstrated that CMIP6 models can be used for regional precipitation extreme studies. Table 1 shows the information of 17 models and their availability for the historical simulations from 1850 to 2014 and future projections from 2015 to 2100 under three Shared Socioeconomic Pathways (SSPs). SSP585, SSP245, and SSP126 represent the high, medium, and low ends of the range of future pathways producing radiative forcings of 8.5 W/m^2, 4.5 W/m2, 2.6 W/m^2 by 2100, respectively (O'Neill et al. 2016). There is one model (NESM3) without SSP245 simulations available and two models (NESM3 and NorESM2-LM) without SSP126 simulations available. Although some models provide more than one ensemble member, only the first ensemble member is used in the analysis. This approach is consistent with previous studies assessing projected changes in precipitation extremes (Akinsanola et al. 2020).

Table 1
Information of the 17 CMIP6 models used in this study.

Model	Horizontal resolution (lat×lon grid numbers)	historical	SSP585	SSP245	SSP126
ACCESS-CM2	144×192	✓	✓	✓	✓
ACCESS-ESM1-5	145×192	✓	✓	✓	✓
BCC-CSM2-MR	160×320	✓	✓	✓	✓
CanESM5	64×128	✓	✓	✓	✓
CESM2	192×288	✓	✓	✓	✓
FGOALS-g3	90×180	✓	✓	✓	✓
GFDL-CM4	180×288	✓	✓	✓	
GFDL-ESM4	180×288	✓	✓	✓	✓
INM-CM5-0	120×180	✓	✓	✓	✓
IPSL-CM6A-LR	143×144	✓	✓	✓	✓
MIROC6	128×256	✓	✓	✓	✓
MPI-ESM1-2-HR	192×384	✓	✓	✓	✓
MPI-ESM1-2-LR	96×192	✓	✓	✓	✓
MRI-ESM2-0	160×320	✓	✓	✓	✓
NESM3	96×192	✓	✓		
NorESM2-LM	96×144	✓	✓	✓	
NorESM2-MM	192×288	✓	✓	✓	✓

2.2 Evaluation data

Precipitation data for the period 1950–2014 is obtained from the 3rd phase Global Soil Wetness Project (GSWP, Kim 2017) to evaluate the CMIP6 models' performance in simulating historical transitions of precipitation extremes. GSWP is a hybrid dataset produced based on a dynamical downscaling of the 20th Century Reanalysis (20CR, Compo et al. 2011) at a spatial resolution of 0.5°×0.5° latitude-longitude grid. Bias corrections are then applied using global observationally-based gridded datasets (such as Global Precipitation Climatology Centre, GPCC; Global Precipitation Climatology Project, GPCP; Climate Prediction Center (CPC) Unified Precipitation Project) to improve the representation of temperature and

precipitation variables (Dirmeyer et al. 2006; Yoshimura and Kanamitsu 2008). This dataset has been used as the primary meteorological forcing in the offline simulations of the Land Surface, Snow and Soil Moisture Model Intercomparison Project (LS3MIP), a CMIP6-Endorsed Model Intercomparison Project (MIP), which is designed to evaluate the land models of current Earth system models and investigate land surface, snow and soil moisture feedback to climate variability and climate change (van den Hurk et al. 2016). Although precipitation bias has been found in many gridded meteorological datasets when compared to in situ observations due to the intrinsic heterogeneity (van den Hurk et al. 2016) and many of gridded datasets show a negative bias in precipitation over the Great Lakes region (Behnke et al. 2016), the application of GSWP in LS3MIP as the primary forcing dataset demonstrates its credibility in representing precipitation variability.

The spatial resolution of gridded datasets can possibly affect the detected precipitation extremes, particularly over regions with complex terrain (Gervais et al. 2014; Herold et al. 2016). However, the Midwest is not as orographically complex as the eastern or western US. Precipitation products at such a spatial resolution have been used to assess precipitation extremes in previous studies (e.g., Donat et al. 2013; Olmo et al. 2020; Zhou et al. 2016). Meanwhile, comparing the GSWP-based results with the high-resolution results in our previous study (Ford et al. 2021), the two datasets show a good agreement in the spatial pattern in transitions of precipitation extremes, although GSWP may lose some spatial details (to be discussed in Section 3). Considering the uncertainty of the precipitation data, another observational precipitation dataset, the gridded CPC unified gauge-based precipitation analysis (Chen et al. 2008; Xie et al. 2010), is also used for the evaluation. The CPC dataset provides daily precipitation at a spatial resolution of 0.5°×0.5° latitude-longitude grid over the contiguous US since 1948.

2.3 Definitions of variability and transitions in precipitation extremes

In this study, precipitation extremes are characterized using the Standardized Precipitation Index (SPI; McKee et al. 1993). SPI is a probability-based index and has been widely used for drought monitoring (Svoboda et al. 2002) and precipitation extremes studies (e.g., Choi et al. 2016; Russo et al. 2013; Wang et al. 2017). It should be noted that there are several limitations of SPI, including the requirement for data quality and length, not being capable of identifying regions that may be more “drought-prone” than others, and possibly misleading large values of short-term SPI in regions with low seasonal precipitation (Hayes et al. 1999), and no consideration of other meteorological conditions closely related to drought. However, due to its simplicity and versatility, SPI has been recommended as a key drought indicator by the World Meteorological Organization (Wilhite 2006) and a universal meteorological drought index by the Lincoln Declaration on Drought (Hayes et al. 2011). In the SPI algorithm, at a given grid cell, long-term (e.g., the historical period 1950–2014 in this study) precipitation data is used to determine the probability density function (PDF) of n-day accumulated precipitation by fitting a gamma distribution. To calculate the SPI for each CMIP6 model, its historical simulation during 1950–2014 is used as the reference to fit the gamma distribution. Then the actual n-day accumulated precipitation on a given day in a given year (in the historical or future period) is expressed as a standardized departure from the PDF. In this study, we

calculate 30-, 90- and 180-day SPI to characterize monthly to seasonal precipitation extremes. We used those three aggregation periods, matching the methods of Ford et al. (2021) to capture variability, change, and transitions at the subseasonal to seasonal timescale. Variability and transitions on shorter timescales (i.e., 30-days) are important for agriculture management and decision making, while those on 90- to 180-day timescales are more relevant for water resource planning. Because the calculation of accumulated precipitation produces missing values for the first n-1 days, the first year (1950) is discarded in our analysis.

We apply two SPI-based metrics developed in Ford et al. (2021) to quantify the transition of precipitation extremes: intra-annual variability and transition. Intra-annual variability is based on the annual maximum SPI and annual minimum SPI within a calendar year. It allows us to quantify the magnitude and duration of extreme precipitation variability of each year. Magnitude is defined as the difference between the annual maximum and minimum SPI; duration is the time span between the two intra-annual extremes, measured in days.

Because the calculation of SPI can essentially erase the seasonal cycle of precipitation, the identified intra-annual variability should be carefully evaluated. First, we compare the annual maximum/minimum precipitation with the actual precipitation when the annual maximum/minimum SPI is identified (Figure S1). The total precipitation associated with the max/min SPI is very similar to the annual max/min precipitation totals. Although SPI-based results are slightly less extreme than the total precipitation-based results (i.e., higher minima and lower maxima), the overall agreement suggests that the SPI-based approach is representative of dry/wet conditions and the magnitude of the seasonal cycle of precipitation.

We then examine the difference in timing between annual maximum (minimum) SPI and accumulated precipitation (Figure S2). For 30-day SPI, most of the domain shows the average difference in timing is within 60 days, suggesting that the identified maxima or minima are still representative of the wet/dry conditions for a certain season. We also see certain differences between the SPI-based results and the actual precipitation, especially over the Northwest. This is mainly because there is relatively strong seasonal variability in precipitation in those regions, with evident dry and wet seasons (Figure S3). For instance, an average amount of precipitation during the dry season can be less than the precipitation amount for an “extreme-dry” period during the wet season. If using actual precipitation for detection, the average dry season will be identified as the annual minimum; if using SPI, the “extreme-dry” wet season will be considered as the annual minimum. Although both are justifiable, an SPI value represents the deviation of the total precipitation from the average or expected value, which speaks to the intensity of the anomaly. Spatially speaking, having the same SPI value in a humid area and a semi-arid area signifies that the total precipitation in the two cities is of equal anomaly or intensity, after having accounted for the difference in background climatology. This eases comparison of precipitation extremes across a large region such as the Midwest, also is the primary reason why SPI has been used frequently for identifying precipitation extremes in previous studies (e.g., Zhang et al. 2009; Mallya et al. 2016;

Onuşluel Gül et al. 2021) and was one of the many reasons SPI was recommended to the WMO as a primary indicator for monitoring meteorological drought worldwide (Hayes et al. 2011).

The transition, or as DeGaetano and Lim (2020) described, the “tail swing”, occurs when SPI moves from at or above + 1.6 to at or below − 1.6, or vice versa. The transition can occur within a single calendar year or across different years. This approach allows us to quantify transition frequency and duration (i.e., how quickly the transition occurred). The frequency of transitions is defined as the number of transitions within a certain period (e.g., the period 1951–2014 used for model evaluation). The duration of a transition is defined as the number of days that elapse between the extreme of one sign and the subsequent extreme of the opposite sign. More details of the transition can be found in Ford et al. (2021). It should be noted that the thresholds ± 1.6 are used for the transition calculation because the value − 1.6 of SPI is the threshold for identifying “extreme drought” in the US drought monitor. We also test the thresholds at ± 0.8, which are used to define “moderate drought”. The identified transitions are more frequent if considering modest extremes, but their spatial patterns are consistent (not shown).

2.4. Quantify future changes in transitions of precipitation extremes

We calculate intra-annual variability and transitions of precipitation extremes for the historical period 1951–2014 from individual CMIP6 models. Due to the different spatial resolutions of CMIP6 models, the calculated metrics are regridded to a common 1.0°×1.0° latitude-longitude grid size, and multimodal ensemble medians are then calculated. Observation-based metrics are calculated using the GSWP and CPC precipitation, and are also regridded to a 1.0°×1.0° latitude-longitude resolution for the evaluation purpose. When calculating the average across the Midwest, we use grid cells within the area 34°~50° N and 80°~100° W of the US. Additionally, to evaluate the performance of individual CMIP6 models and multimodel ensemble median, ranking scores are calculated based on correlation coefficient and relative bias of the climatology of each SPI-based variable (annual maximum SPI, annual minimum SPI, magnitude of intra-annual variability, duration of intra-annual variability, frequency of transitions, duration of dry-to-wet transitions, and duration of wet-to-dry transitions). The correlation coefficient measures the spatial agreement between the observation and model, and relative bias (*RB*) measures the mean error for each model (Eq. 1).

$$RB = \frac{\bar{\mathrm{M}} - \bar{O}}{\bar{O}} \times 100\% \quad (1)$$

where $\bar{M}$ and $\bar{O}$ are climatological mean from the model and observation, respectively. The total ranking score (*RS*) is defined in Eq. 2 according to the method in Kim et al. (2020).

$$RS = 1 - \frac{1}{MNR}\sum_{i=1}^{R}\sum_{j=1}^{N} rank_{i,j}$$

2

where *M* is 18 (the multimodel ensemble median and 17 CMIP6 models), *N* is 3 (the variable derived from 30-, 90-, and 180-day SPI), *R* is 2 (correlation coefficient and relative bias), and $rank_{i,j}$ represents the ranking of the model for the evaluation measure *i* and the SPI-based variable *j*. Values of *RS* closer to 1 indicate better model performance.

For the projected changes in transitions, we calculate the difference between the historical period (1981–2010) and the future period (2071 – 2000 as long-term future) under three SSPs. Two criteria are used to evaluate the statistical significance of the projected change. First, the non-parametric Wilcoxon signed-rank test is used to assess the statistical significance of the multimodel ensemble median (Sillmann et al. 2013). The projected changes are considered “significant” when the Wilcoxon test rejects the null hypothesis at the 5% significance level. Second, the robustness across CMIP6 models is assessed based on inter-model agreement (Chen 2020). The projected changes are considered “robust” when at least 75% of the models agree on the sign of the change.

3. Evaluation Of The Historical Precipitation Extreme Transitions

We first evaluate the climatology of annual maximum and minimum SPI during the period 1951–2014. Figure 1 shows the comparison between GSWP and CMIP6. Although GSWP is a hybrid precipitation product at a relatively coarse resolution, it well represents the spatial distribution of SPI extremes compared to the observations used in Ford et al. (2021) (Figure S4). For the 30-day SPI, the eastern half of the Midwest shows higher values in annual maximum (i.e., wetter) and lower values in annual minimum (i.e., drier), indicating greater shorter-term precipitation variability in this region. For the 90-day and 180-day SPI, the northern regions exhibit a larger intra-annual range, suggesting greater longer-term precipitation variability in those regions. Figure S5 shows the climatology of annual maximum and minimum SPI based on the CPC precipitation dataset, which exhibits a reasonably good agreement with the GSWP-based results in both magnitude and spatial pattern. The major difference is found in the annual minimum 30-day and 90-day SPI. CPC suggests lower values in the southwest, but GSWP and nClimDiv in Ford et al. (2021) suggest lower values in the southeast. Previous studies also discussed the uncertainty among different observational datasets, and concluded that the spread among different observational datasets for most precipitation extreme indices are comparable to the CMIP6 interquartile model spread (Srivastava et al. 2020). CMIP6 somewhat captures the observed spatial pattern of SPI extreme climatologies, except for the annual minimum 90-day SPI. Meanwhile, the multimodel ensemble median of CMIP6 has smoothed spatial variability. For instance, CMIP6 underestimates the dry conditions in the north, where the 180-day annual minimum SPI is relatively low, but overestimates the dry conditions in other regions.

Figure 2 shows the magnitude and duration of intra-annual variability in GSWP and CMIP6. Similar to the finding in SPI extreme climatologies, there is greater intra-annual variability in 30-day SPI over the eastern half of the Midwest. With longer SPI intervals (e.g., 90 days or 180 days), the value of magnitude gradually decreases, and more areas in the north exhibit relatively higher intra-annual variability compared to other regions. CPC agrees with GSWP in the magnitude and duration and intra-annual variability (Figure S6), but the magnitude of the 30-day SPI variability shows relatively high values in the southwest, which are not present in GSWP and Ford et al. (2021). CMIP6 shows a general agreement in the spatial pattern with GSWP, with a pattern correlation of 0.54, 0.47, and 0.61 for 30-day, 90-day, and 180-day SPI, respectively. According to the three observation-based SPI intervals, northern regions (e.g., Wisconsin, Minnesota, and North Dakota) have a relatively short duration of intra-annual variability, suggesting the transitions between wet and dry events usually occur within a shorter time in those regions. For instance, a transition from extreme dry to extreme wet conditions occurs on average within four months in northern Wisconsin. CMIP6 does not capture the duration of intra-annual variability at 30-day and 90-day SPI, but shows a good agreement with GSWP for 180-day SPI.

Figure 3 shows the frequency of transition during the period 1951–2014. For 30-day SPI, more frequent transitions occur over the eastern half of the Midwest, especially in the Great Lakes region, with a return interval of less than a year. When SPI is calculated at a longer interval (e.g., 180 days), the northern states, such as Minnesota and North Dakota, also exhibit high transition frequency, with a return interval of about 2.7 years. Again, CPC shows a reasonably good agreement with the GSWP in both magnitude and spatial pattern of the frequency (Figure S7). Generally, CMIP6 well represents the observed high frequency of 30-day SPI transitions in the east, and the high frequency of 90-day and 180-day SPI transitions in the north and the Great Lakes region. The pattern correlation between CMIP6 and GSWP is 0.58, 0.47, and 0.35 for 30-day, 90-day, and 180-day SPI transitions, respectively. However, CMIP6 exhibits less spatial variability than GSWP. Although CMIP6 agrees with GSWP in the regions with a higher frequency of transitions, it overestimates the frequency in the rest areas of the Midwest.

The duration of transitions is closely related to the frequency - a higher frequency generally corresponds to quicker transitions. Therefore, the duration of transitions from extreme dry (wet) to extreme wet (dry) shows a consistent pattern with the frequency (Figure S8). The shortest 30-day SPI transitions occur in the east and the Great Lakes regions, where transitions of precipitation extremes only take 3–4 months. The 180-day SPI shows that the shortest transitions also appear in the north, such as Minnesota and Dakotas. We also note some differences between the dry-to-wet and wet-to-dry transitions. The 180-day SPI highlights the southwest part of the region, which exhibits relatively quick dry-to-wet transitions (Figure S8c), which is not shown in the wet-to-dry transitions (Figure S8i). Similar to the performance in simulating transition frequency, CMIP6 captures the spatial pattern of the duration but with overall less variability in many regions.

Furthermore, we evaluate the temporal evolution of SPI extremes. Figure 4 shows the time series of annual maximum and minimum SPI averaged over the Midwest. Although there is little agreement in inter-annual variability of the SPI extremes between GSWP and CMIP6, we do find the general trends are

consistent in these two datasets. During the historical period 1951–2014, observations show a significant increase in annual maximum SPI. The rate of increase is larger for longer-term SPI intervals. CMIP6 also exhibits a significant positive trend in annual maximum SPI but at a lower rate. Both observations and CMIP6 show a decrease in the 30-day annual minimum SPI (i.e., increasing dry extremes), and an increase in the 90- and 180-day SPI annual minimums (i.e., decreasing dry extremes); however, these trends are not statistically significant.

Overall, the multimodel ensemble median of CMIP6 shows good agreement with the observations with respect to the spatial patterns of intra-annual variability and transitions of precipitation extremes. Although biases are noted in some regions, the models are capable of representing the climatologies of transitions and the general trends of SPI extremes in the Midwest. Moreover, we examine the performance of individual CMIP6 models. The multimodel ensemble median consistently outperforms most of the models throughout all the SPI-based variables (Table S1). We also find there is no evident difference in the projected changes between the multimodel ensemble from all available models and the multimodel ensemble from best performance models (e.g., top 5) (not shown). Therefore, to maintain a consistent set of models in the historical and future analysis, we chose to use the median values based on simulations from all CMIP6 models in both cases.

4. Projected Changes In Transitions Of Precipitation Extremes

4.1 Changes in SPI extremes and intra-annual variability

From 2015 to 2100, all three scenarios show a significant increase in annual maximum SPI over the Midwest, indicating that the intensity of wet events is projected to increase in the future (Fig. 4). Among the three scenarios, SSP585 shows the greatest increase. The annual maximum 30-day SPI averaged across the Midwest is about 2.07 during the reference period 1981–2010. By the end of the century (2071–2100), the annual maximum SPI is projected to increase by 0.54, approximately 26% relative to the baseline. For reference, the regional-average annual maximum 30-day SPI during the extreme flooding of 2019 was 2.37. Although SSP245 and SSP126 also exhibit a rapid increase at the early stage of the 21st century, the rate of increase moderates from 2040 to the end of the century, likely due to less projected warming as a result of future climate mitigation efforts applied to these scenarios (O'Neill et al. 2016). By the end of the century, the annual maximum 30-day SPI is estimated to increase by 18% and 14% in SSP245 and SSP126, respectively. Similar to the historical trends, the projected change in annual minimum SPI depends on the time interval of the SPI investigated. The 30-day SPI shows a significant decrease in the Midwest, suggesting the short-term dry events will get more intense. The average annual minimum 30-day SPI is -2.35 during the reference period, and is projected to decrease by approximately 15% (-0.35) by the period 2071–2100. For reference, the region-average annual minimum 30-day SPI during the drought year of 2012 was − 2.82. SSP245 and SSP126 exhibit a negative trend in 30-day SPI, however, which is not statistically significant. For the 90-day or 180-day SPI, the trend of annual minimum SPI is relatively small and mostly not significant, which broadly supports the hypothesis that seasonal

drought in this region will not systematically increase in response to the greenhouse gas forcing (e.g., Cook et al. 2020).

Figure 5 shows the spatial distributions of projected changes in annual maximum and minimum SPI in the Midwest by the end of the century. The annual maximum SPI is projected to increase across the Midwest in all three scenarios, with the greatest increase in SSP585. Spatially, the intensification of wet conditions is stronger in the northern states and the Great Lakes region. The annual minimum 30-day and 90-day SPI shows a significant decrease in SSP585, especially over the western half of the Midwest. We also see a slight decrease over the southwest in SSP245 and SSP126, and a slight increase in 180-day SPI in some areas of the west. However, no significant changes are found in large areas of the Midwest in SSP245 and SSP126 with longer SPI intervals. This agrees with the regional average time series (Fig. 4), indicating little change in the intensity of future seasonal to multi-season meteorological droughts over the Midwest.

Due to the increased annual maximum SPI and decreased annual minimum SPI, the magnitude of intra-annual variability shows a significant increase in most of the areas in the Midwest by the end of the century (Fig. 6). The greatest increase is found in the northern half of the study area for the 30-day SPI under the SSP585 scenario. Meanwhile, we note that there is no significant change in the duration of intra-annual variability (Figure S9). From the historical perspective (Fig. 2), the northern states already have a relatively short duration of intra-annual variability. Therefore, the projected increase in magnitude would pose a higher risk of precipitation extremes in those regions.

4.2 Changes in transition

Figure 7 shows the projected changes in the frequency of precipitation transitions. The 30-day SPI suggests significantly more transitions will occur across the Midwest by the end of the century in SSP585 and SSP245. The most prominent increase can be found in 30-day SPI over the Great Lakes regions and the northern Midwest, including Minnesota, Wisconsin, Illinois, Indiana, and Michigan, where at least one more transition will occur every two years. The changes account for about 30% increase compared to the historical transition frequency. It should be noted that the Great Lakes and the north already have higher transition frequency than other areas of the Midwest during the historical period. The greater increase in future transition frequency would further highlight the vulnerability of those regions to climate change. When precipitation extremes are quantified using a longer-interval SPI, there is a slight increase in transition frequency in the western half of the Midwest in SSP585 and no significant changes in the other two scenarios. Additionally, we examine the projected changes related to the definition of precipitation extremes (section 2.3). Figure S10 shows the projected changes in the frequency of transitions based on three sets of thresholds (± 1.6, ± 1.2, and ± 0.8). They are used because − 1.6, -1.2, and − 0.8 are used to define extreme, severe, and moderate droughts, respectively, according to the drought classification of US drought monitoring. The spatial patterns of the project changes among the three sets of thresholds are consistent. If including severe/moderate extremes, the magnitude of the projected increase in transition frequency is much lower than the magnitude with considering “extreme” extremes only, especially for the

30- and 90-day SPI. This suggests that there are more frequent transitions between extreme wet/dry conditions, but fewer transitions between moderate wet/dry conditions.

The increased frequency can correspond to a shortened duration of precipitation transitions (Fig. 8). Both dry-to-wet and wet-to-dry transitions are projected to become more rapid across the Midwest under a warming climate. Historically, the transitions would take around 3 months over the Great Lakes region (Figure S8). Under a warming climate, the reduced duration is about 20 days in those regions. Although no significant changes in transition frequency are found in SSP245 and SSP126 for 180-day SPI, we note significantly reduced transition durations in some regions (e.g., Illinois). Therefore, future warming may not affect the total number of transitions between long-term droughts and wet conditions, but significantly accelerates the transitions between the extremes. The unaltered transition frequency with reduced transition duration also imply that the long-term extremes may last longer in the future, however, which is out of the scope of this study and will be investigated in our future work.

4.3 Changes in seasonality

We examine the seasonality of the transitions averaged across the Midwest during the historical period 1981–2010 and the future period 2071–2100 under the SSP585 scenario. Because the 90-day and 180-day SPI is based on the accumulated total precipitation over three months and six months, respectively, their seasonality has been largely smoothed out. Therefore, our analysis is only focused on the 30-day SPI. Figure 9 shows the frequency of maximum and minimum 30-day SPI that is identified in different months. Historically, GSWP and CMIP6 show a good agreement. A slight difference is found in annual minimum SPI during summer, which may explain the discrepancy in the duration of intra-annual variability discussed in section 3. The frequency of SPI extremes is evenly distributed throughout the year. In other words, no clear seasonality is seen in the occurrence of annual maximum and minimum SPI. By the end of the century, more annual maximum SPI tends to occur during the cold season (e.g., from December to April), and more annual minimum SPI tends to occur during the warm season (e.g., from July to September). The projected changes in the seasonality of SPI extremes demonstrate a potential wet-spring-dry-summer pattern in a warming climate, which is also documented in previous studies (Byun and Hamlet 2018; Dai et al. 2016; Hamlet et al. 2019). This is also consistent with cool-season warming in the northern parts of the domain, where temperature currently limits winter precipitation.

Figure 10 shows the seasonality of transitions between extreme wet and dry conditions. Similar to the SPI extremes, neither wet-to-dry nor dry-to-wet transitions show evident seasonality during the historical period. Under the SSP585 scenario, there are more wet-to-dry transitions occurring in late spring or early summer, and more dry-to-wet transitions happening in late fall or early winter. As the duration of the transition is projected to decrease in the future, the transitions would only take 2–3 months. Consequently, slightly more wet-to-dry transitions end in summer, and more dry-to-wet transitions end in winter/spring. Combining with the results discussed in section 4.2, the projected changes in seasonality suggest that more frequent transitions from a wet spring to a dry summer (or from a dry fall to a wet

winter/spring) will occur in the Midwest, and, generally, the wet and dry conditions between the transitions are projected to be more intense compared to the historical period.

5. Summary And Conclusions

This study investigates the historical and future variability of and transitions between precipitation extremes in the Midwest using state-of-the-art climate models in CMIP6. We find significantly increased magnitude of precipitation extremes and increased frequency of transitions, which could have substantial socio-economic and environmental impacts in the Midwest. Similar results about future wet and dry extremes have been documented in recent studies of the CMIP6 projections (e.g., Akinsanola et al. 2020; Cook et al. 2020). Observation-based assessments have suggested that increased precipitation variability and systematic warming have important implications for flood risk and conjunctive water management (Hamlet and Lettenmaier 2007). The projected increase in annual maximum SPI suggests heavy precipitation is expected to be more intense, possibly leading to increased flood risk and issues with excessively wet soils (Scoccimarro and Gualdi 2020; Byun et al. 2019). Due to the large area of agricultural land in the Midwest, the increased heavy precipitation is also likely to drive more nutrient runoff to surface water bodies (Coffey et al. 2018; Motew et al. 2018), and augment long-standing soil erosion issues in the region (Thaler et al. 2021). The increased flood risk also poses challenges for the drainage system in urban areas (Yazdanfar and Sharma 2015), particularly those with undersized systems and/or combined sewer overflows.

Meanwhile, the projected decrease in annual minimum SPI indicates that future dry conditions will get drier, exposing the agricultural regions to potential economic losses due to drought (Ukkola et al. 2020). Irrigation has often been proposed as a climate adaptation strategy to improve crop resilience to future changes in drought risk (e.g., Li et al. 2020). However, along with being cost-prohibitive, widespread adoption of irrigation, especially in the currently majority non-irrigated agricultural lands in the Midwest, could exacerbate water supply issues for municipal or commercial use in times of prolonged drought. Soil and water conservation strategies are also vital adaptation measures for Midwest agriculture, and are becoming increasingly important to boost resilience to drought and reduce soil erosion and nutrient runoff from increasing precipitation intensity.

It is important to note that the sequencing of precipitation extremes can greatly determine the magnitude of associated impacts. For example, a 30-day dry extreme that follows a prolonged wet period will have less socio-economic impacts than the same extreme following a near-normal or prolonged dry period. Similarly, conditions preceding wet extremes such as soil moisture conditions, reservoir levels, and streamflow can greatly impact the extent of flood damage associated with wet extremes. Although it is beyond the scope of this study, further impact-focused research is necessary to better recognize and communicate the implications of changing Midwest precipitation extremes for drought and flood impact preparedness, adaptation, and management.

We also find more frequent transitions of precipitation extremes, particularly transitions from wet spring to dry summer in the Midwest. Observation-based studies also document a wetting trend during the early growing season and a drying trend during the late growing season in the Midwest (Dai et al. 2015). Such a transition would seriously impair crop production, especially for the rainfed crops, which dominate agriculture in the eastern Midwest. Excess precipitation and flooding in spring can cause widespread planting delays for both commodity and annual specialty crops, soil compaction, poor seed germination, higher fungus, and bacterial disease incidence, and lead to issues with nutrient loss and soil erosion (Rao and Yi, 2003; Kleinman et al. 2006). Concurrently, even 30- or 90-day drought, if aligned with crop pollination and/or grain/fruit formation periods, can lead to yield decreases or crop failure (Westcott et al. 2005; Rippey et al. 2015). The results of this study show projected increases in the speed of transitions between extremely wet and dry conditions, suggesting overall less time for preparation and management of the hazard impacts.

Like other precipitation extreme studies (such as Akinsanola et al. 2020, Srivastava et al. 2020), this study is based on climate projections from state-of-the-art climate models in CMIP6. However, we need to acknowledge certain limitations of the current analysis. First, the dry bias in the central US has been a long-standing issue in CMIP5 and CMIP6 models (Al-Yaari et al. 2019; Srivastava et al. 2020). The SPI-based analysis can somewhat avoid the influence of the mean bias, but associated uncertainty in precipitation distribution may still affect the identified precipitation extremes (Pierce et al. 2015). Second, the springtime extreme precipitation over the central US is primarily controlled by mesoscale convective systems (Feng et al. 2016). However, current CMIP6 models still are not able to resolve these mesoscale convective systems due to their coarse spatial resolutions (Ridder et al. 2021). Therefore, it is necessary to investigate the impacts of bias correction and high-resolution dynamical downscaling on the transitions of precipitation extremes. Meanwhile, although dynamical downscaling can provide more useful information for regional impact studies due to its higher spatial resolution, uncertainties related to regional climate models (RCMs) cannot be ignored. Our previous study found that different RCMs with the same GCM boundary conditions can lead to opposite changes in precipitation extremes (Chen and Ford 2021). Some studies even show worse performance in dynamic downscaling than GCMs (e.g., Mishra et al. 2018). Moreover, coarse-resolution (e.g., 12–50 km) and high-resolution (e.g., convection-permitting resolution, < 5 km) RCMs may lead to inconsistent rainfall intensity (Kendon et al. 2017). Therefore, when dynamically downscaled CMIP6 climate data becomes available, it will be worthwhile to evaluate the added value of downscaling in precipitation extremes compared to the GCMs.

It is expected that the intensity of heavy precipitation would scale with the change in air temperature (Held and Soden 2006). Therefore, we see significantly increased annual maximum SPI with the greatest increase in the SSP585 scenario, which corresponds to the greatest temperature increase (Cook et al. 2020). Meanwhile, a warmer atmosphere would take longer to replenish its moisture between storms (Shiu et al. 2012), potentially leading to longer dry spells and intensified drought conditions. However, identifying the mechanisms that result in projected more frequent and rapid transitions of precipitation extremes will be a focal point in our future work.

Despite the potential future risks of intensified precipitation extremes and more frequent transitions over the Midwest, we note considerable differences in the projected changes among different scenarios. The projected increase in magnitude and frequency of precipitation extreme transitions can be largely avoided under a lower-emission scenario (Figs. 5–8). Aligning with previous literature that has explored the impacts of 0.5°C less global warming on climate extremes (such as Zhang et al. 2018; King and Karoly 2017; Hoegh-Guldberg et al. 2018), this study highlights the importance of climate mitigation efforts in reducing the risks of extreme events in the Midwest.

In summary, this study investigates the projected changes in transitions of precipitation extremes in the Midwest using climate simulations from 17 CMIP6 models. Two SPI-based metrics, intra-annual variability and transition adopted from Ford et al. (2021), are used to quantify the magnitude, duration, and frequency of transitions between wet and dry extremes. The evaluation with the observation-based precipitation dataset suggests the multimodel ensemble median of CMIP6 can reasonably represent the spatial patterns of the SPI extremes and transitions during the historical period. For instance, using 30-day SPI, which depicts short-term (e.g., monthly) precipitation variability, we see greater intra-annual variability and higher frequency of transitions in the eastern half of the Midwest, especially in the Great Lakes region. With longer SPI intervals, which represent longer-term (e.g., seasonal) precipitation variability, the northern areas exhibit greater magnitude and shorter duration of intra-annual variability, and higher frequency of transitions.

Climate projections suggest significantly intensified wet extremes across the Midwest by the end of the century, with a greater increase in the north and the Great Lakes region. The short-term SPI also shows intensified dry extremes over the western half of the Midwest. Consequently, there is significantly increased intra-annual variability in most of the areas in the Midwest compared to the historical period. Meanwhile, a warming climate also leads to more frequent and rapid transitions between the wet and dry extreme events, especially over the Great Lakes regions and the northern states. Seasonality analysis further reveals that more frequent transitions from a wet spring to a dry summer (or from a dry fall to a wet winter/spring) will occur in the Midwest. The difference among three scenarios, including SSP585, SSP245, and SSP126, indicates that the intensified precipitation extremes and accelerated transitions can be greatly alleviated under a lower emission scenario, and highlights the importance of effective climate action in the long-term development of climate-vulnerable regions in the Midwest.

Declarations

Acknowledgements

This work was supported by NOAA Contract NA18OAR4310253B, with support from the Illinois Farm Bureau. We acknowledge the World Climate Research Programme, which, through its Working Group on Coupled Modelling, coordinated and promoted CMIP6. We thank the climate modeling groups for producing and making available their model output, the Earth System Grid Federation (ESGF) for archiving the data and providing access, and the multiple funding agencies that support CMIP6 and

ESGF. All CMIP6 data are available from https://esgf-node.llnl.gov/projects/cmip6/. The CPC US Unified Precipitation data provided by the NOAA/OAR/ESRL PSL, Boulder, Colorado, USA, from their website at https://psl.noaa.gov/data/gridded/data.unified.daily.conus.html. We would like to thank Dr. David Kristovich for his review of this manuscript. The authors declare that there is no conflict of interest. We also thank the reviewers for their constructive and thoughtful comments, which helped us improve this manuscript.

References

1. Akinsanola, A. A., G. J. Kooperman, K. A. Reed, A. G. Pendergrass, and W. M. Hannah, 2020: Projected changes in seasonal precipitation extremes over the United States in CMIP6 simulations. Environmental Research Letters, doi:10.1088/1748-9326/abb397.
2. Akinsanola, A.A., Kooperman, G.J., Pendergrass, A.G., Hannah, W.M., Reed, K.A., 2020. Seasonal representation of extreme precipitation indices over the United States in CMIP6 present-day simulations. Environmental Research Letters, **15**, 094003. doi:10.1088/1748-9326/ab92c1
3. Al-Yaari, A., A. Ducharne, F. Cheruy, W. T. Crow, and J. P. Wigneron, 2019: Satellite-based soil moisture provides missing link between summertime precipitation and surface temperature biases in CMIP5 simulations over conterminous United States. Sci. Rep., **9**, 1657, doi:10.1038/s41598-018-38309-5.
4. Angel, J. and Coauthors, 2018: Midwest. In Impacts, Risks, and Adaptation in the United States: Fourth National Climate Assessment, Volume II [Reidmiller, D.R., C.W. Avery, D.R. Easterling, K.E. Kunkel, K.L.M. Lewis, T.K. Maycock, and B.C. Stewart (eds.)]. U.S. Global Change Research Program, Washington, DC, USA, pp. 872–940. doi: 10.7930/NCA4.2018.CH21.
5. Bador, M., M. G. Donat, O. Geoffroy, and L. V. Alexander, 2018: Assessing the robustness of future extreme precipitation intensification in the CMIP5 ensemble. J. Clim., **31**, 6505–6525, doi:10.1175/JCLI-D-17-0683.1.
6. Basso, B., Martinez-Feria, R.A., Rill, L., and J.T. Ritchie, 2021: Contrasting long-term temperature trends reveal minor changes in projected potential evapotranspiration in the US Midwest. Nature Comm., **12**, 1476, doi: 10.1038/s41467-021-21763-7.
7. Berhane, T. M., C. R. Lane, S. G. Mengistu, J. Christensen, H. E. Golden, S. Qiu, Z. Zhu, and Q. Wu, 2020: Land-Cover Changes to Surface-Water Buffers in the Midwestern USA: 25 Years of Landsat Data Analyses (1993–2017). Remote Sens (Basel), **12**, 754, doi:10.3390/rs12050754.
8. Byun, K., Chiu, C.-M., Hamlet, A.F., 2019. Effects of 21st century climate change on seasonal flow regimes and hydrologic extremes over the Midwest and Great Lakes region of the US. Sci. Total Environ., **650**, 1261–1277. doi:10.1016/j.scitotenv.2018.09.063
9. Byun, K., Hamlet, A.F., 2018. Projected changes in future climate over the Midwest and Great Lakes region using downscaled CMIP5 ensembles. Int. J. Climatol., **38**, e531–e553. doi:10.1002/joc.5388
10. Chen, L., Ford, T.W., 2021. Effects of 0.5°C less global warming on climate extremes in the contiguous United States. Clim. Dyn., 57, 303–319. doi:10.1007/s00382-021-05717-9

11. Chen, M., W. Shi, P. Xie, V. B. S. Silva, V. E. Kousky, R. Wayne Higgins, and J. E. Janowiak, 2008: Assessing objective techniques for gauge-based analyses of global daily precipitation. J. Geophys. Res., **113**, D04110, doi:10.1029/2007JD009132.
12. Choi, Y.-W., and Coauthors, 2016: Future changes in drought characteristics over South Korea using multi regional climate models with the standardized precipitation index. Asia-Pacific J Atmos Sci, **52**, 209–222, doi:10.1007/s13143-016-0020-1.
13. Christian, J., K. Christian, and J. B. Basara, 2015: Drought and Pluvial Dipole Events within the Great Plains of the United States. J. Appl. Meteor. Climatol., **54**, 1886–1898, doi:10.1175/JAMC-D-15-0002.1.
14. Coffey, R., M. J. Paul, J. Stamp, A. Hamilton, and T. Johnson, 2019: A review of water quality responses to air temperature and precipitation changes 2: nutrients, algal blooms, sediment, pathogens. J. Am. Water Resour. Assoc., **55**, 844–868, doi:10.1111/1752-1688.12711.
15. Cohen, J., 2016: An observational analysis: Tropical relative to Arctic influence on midlatitude weather in the era of Arctic amplification. Geophys. Res. Lett., **43**, 5287–5294, doi:10.1002/2016GL069102.
16. Compo, G. P., and Coauthors, 2011: The twentieth century reanalysis project. Q.J Royal Met. Soc., **137**, 1–28, doi:10.1002/qj.776.
17. Cook, B. I., J. S. Mankin, K. Marvel, A. P. Williams, J. E. Smerdon, and K. J. Anchukaitis, 2020: Twenty-first century drought projections in the CMIP6 forcing scenarios. Earth's Future, **8**, doi:10.1029/2019EF001461.
18. Dai, S., M. D. Shulski, K. G. Hubbard, and E. S. Takle, 2016: A spatiotemporal analysis of Midwest US temperature and precipitation trends during the growing season from 1980 to 2013. Int. J. Climatol., **36**, 517–525, doi:10.1002/joc.4354.
19. DeGaetano, A. T., and L. Lim, 2020: Declining U.S. regional and continental trends in intra-annual and interannual extreme temperature swings. Int. J. Climatol., **40**, 2830–2844, doi:10.1002/joc.6369.
20. Dirmeyer, P. A., X. Gao, M. Zhao, Z. Guo, T. Oki, and N. Hanasaki, 2006: GSWP-2: Multimodel Analysis and Implications for Our Perception of the Land Surface. Bull. Amer. Meteor. Soc., **87**, 1381–1398, doi:10.1175/BAMS-87-10-1381.
21. Donat, M.G., Alexander, L.V., Yang, H., Durre, I., Vose, R., Dunn, R.J.H., Willett, K.M., Aguilar, E., Brunet, M., Caesar, J., Hewitson, B., Jack, C., Klein Tank, A.M.G., Kruger, A.C., Marengo, J., Peterson, T.C., Renom, M., Oria Rojas, C., Rusticucci, M., Salinger, J., Kitching, S., 2013. Updated analyses of temperature and precipitation extreme indices since the beginning of the twentieth century: The HadEX2 dataset. J. Geophys. Res. Atmos., **118**, 2098–2118. doi:10.1002/jgrd.50150
22. Feng, Z., L. R. Leung, S. Hagos, R. A. Houze, C. D. Burleyson, and K. Balaguru, 2016: More frequent intense and long-lived storms dominate the springtime trend in central US rainfall. Nat. Commun., **7**, 13429, doi:10.1038/ncomms13429.
23. Ficklin, D. L., J. T. Maxwell, S. L. Letsinger, and H. Gholizadeh, 2015: A climatic deconstruction of recent drought trends in the United States. Environmental Research Letters, **10**, 044009,

doi:10.1088/1748-9326/10/4/044009.

24. Ford, T. W., L. Chen, and J. T. Schoof, 2020: Variability and transitions in precipitation extremes in the midwest united states. J. Hydrometeor, doi:10.1175/JHM-D-20-0216.1.
25. Gervais, M., Tremblay, L.B., Gyakum, J.R., Atallah, E., 2014. Representing Extremes in a Daily Gridded Precipitation Analysis over the United States: Impacts of Station Density, Resolution, and Gridding Methods. J. Clim., **27**, 5201–5218. doi:10.1175/JCLI-D-13-00319.1
26. Hamlet, A.F., Byun, K., Robeson, S.M., Widhalm, M., Baldwin, M., 2019. Impacts of climate change on the state of Indiana: ensemble future projections based on statistical downscaling. Climatic Change, **163**, 1881–1895. doi:10.1007/s10584-018-2309-9
27. Hamlet, A.F., Lettenmaier, D.P., 2007. Effects of 20th century warming and climate variability on flood risk in the western U.S. Water Resour. Res., **43**. doi:10.1029/2006WR005099
28. Hayes, M., Svoboda, M., Wall, N., Widhalm, M., 2011. The lincoln declaration on drought indices: universal meteorological drought index recommended. Bull. Amer. Meteor. Soc., **92**, 485–488. doi:10.1175/2010BAMS3103.1
29. Hayes, M.J., Svoboda, M.D., Wilhite, D.A., Vanyarkho, O.V., 1999. Monitoring the 1996 drought using the standardized precipitation index. Bull. Amer. Meteor. Soc., **80**, 429–438. doi:10.1175/1520-0477(1999)080<0429:MTDUTS>2.0.CO;2
30. Held, I. M., and B. J. Soden, 2006: Robust responses of the hydrological cycle to global warming. J. Clim., **19**, 5686–5699, doi:10.1175/JCLI3990.1.
31. Herold, N., Behrangi, A., Alexander, L.V., 2017. Large uncertainties in observed daily precipitation extremes over land. J. Geophys. Res. Atmos., **122**, 668–681. doi:10.1002/2016JD025842
32. Hirschi, M., Seneviratne, S.I., Alexandrov, V., Boberg, F., Boroneant, C., Christensen, O.B., Formayer, H., Orlowsky, B., Stepanek, P., 2011. Observational evidence for soil-moisture impact on hot extremes in southeastern Europe. Nature Geoscience, **4**, 17–21.
33. van den Hurk, B., and Coauthors, 2016: LS3MIP (v1.0) contribution to CMIP6: the Land Surface, Snow and Soil moisture Model Intercomparison Project – aims, setup and expected outcome. Geosci. Model Dev., **9**, 2809–2832, doi:10.5194/gmd-9-2809-2016.
34. Kendon, E.J., Ban, N., Roberts, N.M., Fowler, H.J., Roberts, M.J., Chan, S.C., Evans, J.P., Fosser, G., Wilkinson, J.M., 2017. Do Convection-Permitting Regional Climate Models Improve Projections of Future Precipitation Change? Bull. Amer. Meteor. Soc., **98**, 79–93. doi:10.1175/BAMS-D-15-0004.1
35. Kim, H., 2017: Global Soil Wetness Project Phase 3 Atmospheric Boundary Conditions (Experiment 1). Data Integration and Analysis System (DIAS). https://doi.org/10.20783/DIAS.501.
36. Kim, M., and Coauthors, 2020: Performance evaluation of CMIP5 and CMIP6 models on heatwaves in Korea and associated teleconnection patterns. J. Geophys. Res. Atmos., **125**, e2020JD032583, doi:10.1029/2020JD032583.
37. King, A. D., and D. J. Karoly, 2017: Climate extremes in Europe at 1.5 and 2 degrees of global warming. Environmental Research Letters, **12**, 114031, doi:10.1088/1748-9326/aa8e2c.

38. Kleinman, P. J. A., M. S. Srinivasan, C. J. Dell, J. P. Schmidt, A. N. Sharpley, and R. B. Bryant, 2006: Role of rainfall intensity and hydrology in nutrient transport via surface runoff. J. Environ. Qual., **35**, 1248–1259, doi:10.2134/jeq2006.0015.

39. Li, Y., Guan, K., Peng, B., Franz, T.E., Wardlow, B., Pan, M., 2020. Quantifying irrigation cooling benefits to maize yield in the US Midwest. Glob. Chang. Biol., **26**, 3065–3078. doi:10.1111/gcb.15002

40. Liu, L., and B. Basso, 2020: Impacts of climate variability and adaptation strategies on crop yields and soil organic carbon in the US Midwest. PLoS ONE, **15**, e0225433, doi:10.1371/journal.pone.0225433.

41. Loecke, T. D., A. J. Burgin, D. A. Riveros-Iregui, A. S. Ward, S. A. Thomas, C. A. Davis, and M. A. S. Clair, 2017: Weather whiplash in agricultural regions drives deterioration of water quality. Biogeochemistry, **133**, 7–15, doi:10.1007/s10533-017-0315-z.

42. Mallya, G., Mishra, V., Niyogi, D., Tripathi, S., Govindaraju, R.S., 2016. Trends and variability of droughts over the Indian monsoon region. Weather and Climate Extremes, **12**, 43–68. doi:10.1016/j.wace.2016.01.002

43. McKee, T. B., N. J. Doesken, and J. Kleist, 1993: The relationship of drought frequency and duration to time scales. *Proceedings of the 8th Conference on Applied Climatology*, **17**, 179–183.

44. Mishra, S.K., Sahany, S., Salunke, P., 2017. CMIP5 vs. CORDEX over the Indian region: how much do we benefit from dynamical downscaling? Theoretical and Applied Climatology, **133**, 1–9. doi:10.1007/s00704-017-2237-z

45. Mo, K.C., and D.P. Lettenmaier, 2018: Drought variability and trends over the Central United States in the instrumental record. J. Hydrometeorol., **19**, 1149–1166, doi: 10.1175/JHM-D-0225.1.

46. Motew, M., E. G. Booth, S. R. Carpenter, X. Chen, and C. J. Kucharik, 2018: The synergistic effect of manure supply and extreme precipitation on surface water quality. Environmental Research Letters, **13**, 044016, doi:10.1088/1748-9326/aaade6.

47. O'Neill, B. C., and Coauthors, 2016: The scenario model intercomparison project (scenariomip) for CMIP6. Geosci. Model Dev., **9**, 3461–3482, doi:10.5194/gmd-9-3461-2016.

48. Olmo, M., Bettolli, M.L., Rusticucci, M., 2020. Atmospheric circulation influence on temperature and precipitation individual and compound daily extreme events: Spatial variability and trends over southern South America. Weather and Climate Extremes, **29**, 100267. doi:10.1016/j.wace.2020.100267

49. Onuşluel Gül, G., Gül, A., Najar, M., 2021. Historical evidence of climate change impact on drought outlook in river basins: analysis of annual maximum drought severities through daily SPI definitions. Nat. Hazards, **110**, 1389–1404. doi:10.1007/s11069-021-04995-0

50. Pierce, D. W., D. R. Cayan, E. P. Maurer, J. T. Abatzoglou, and K. C. Hegewisch, 2015: Improved bias correction techniques for hydrological simulations of climate change*. J. Hydrometeor, **16**, 2421–2442, doi:10.1175/JHM-D-14-0236.1.

51. Rao, R., and Y. Li, 2003: Management of flooding effects on growth of vegetable and selected field crops. Horttechnology, **13**, 610–616, doi:10.21273/HORTTECH.13.4.0610.

52. Ridder, N. N., A. J. Pitman, and A. M. Ukkola, 2021: Do CMIP6 climate models simulate global or regional compound events skillfully? Geophys. Res. Lett., **48**, doi:10.1029/2020GL091152.
53. Rippey, B. R., 2015: The U.S. drought of 2012. Weather and Climate Extremes, **10**, 57–64, doi:10.1016/j.wace.2015.10.004.
54. Russo, S., A. Dosio, A. Sterl, P. Barbosa, and J. Vogt, 2013: Projection of occurrence of extreme dry-wet years and seasons in Europe with stationary and nonstationary Standardized Precipitation Indices. J. Geophys. Res. Atmos., **118**, 7628–7639, doi:10.1002/jgrd.50571.
55. Scoccimarro, E., and S. Gualdi, 2020: Heavy Daily Precipitation Events in the CMIP6 Worst-Case Scenario: Projected Twenty-First-Century Changes. J. Clim., **33**, 7631–7642, doi:10.1175/JCLI-D-19-0940.1.
56. Seneviratne, S.I. and Coauthors, 2012: Changes in climate extremes and their impacts on the natural physical environment. In: Managing the Risks of Extreme Events and Disasters to Advance Climate Change Adaptation [Field, C.B., V. Barros, T.F. Stocker, D. Qin, D.J. Dokken, K.L. Ebi, M.D. Mastrandrea, K.J. Mach, G.-K. Plattner, S.K. Allen, M. Tignor, and P.M. Midgley (eds.)]. A Special Report of Working Groups I and II of the Intergovernmental Panel on Climate Change (IPCC). Cambridge University Press, Cambridge, UK, and New York, NY, USA, pp. 109–230.
57. Shiu, C.-J., S. C. Liu, C. Fu, A. Dai, and Y. Sun, 2012: How much do precipitation extremes change in a warming climate? Geophys. Res. Lett., **39**, doi:10.1029/2012GL052762.
58. Sillmann, J., V. V. Kharin, F. W. Zwiers, X. Zhang, and D. Bronaugh, 2013: Climate extremes indices in the CMIP5 multimodel ensemble: Part 2. Future climate projections. J. Geophys. Res. Atmos., **118**, 2473–2493, doi:10.1002/jgrd.50188.
59. Srivastava, A., R. Grotjahn, and P. A. Ullrich, 2020: Evaluation of historical CMIP6 model simulations of extreme precipitation over contiguous US regions. Weather and Climate Extremes, **29**, 100268, doi:10.1016/j.wace.2020.100268.
60. Svoboda, M., and Coauthors, 2002: The drought monitor. Bull. Amer. Meteor. Soc., **83**, 1181–1190, doi:10.1175/1520-0477-83.8.1181.
61. Tang, B., Hu, W., Duan, A., 2021. Future Projection of Extreme Precipitation Indices over the Indochina Peninsula and South China in CMIP6 Models. J. Clim., **34**, 8793–8811. doi:10.1175/JCLI-D-20-0946.1
62. Thaler, E.A., Larsen, I.J., and Q. Yu, 2021: The extent of soil loss across the US Corn Belt. *Proc. Natl. Acad. Sci. U.S.A.*, **118**, e1922375118, doi:10.1073/pnas.1922375118.
63. Ukkola, A. M., M. G. De Kauwe, M. L. Roderick, G. Abramowitz, and A. J. Pitman, 2020: Robust future changes in meteorological drought in CMIP6 projections despite uncertainty in precipitation. Geophys. Res. Lett., doi:10.1029/2020GL087820.
64. Vose, R. S., and Coauthors, 2014: Improved historical temperature and precipitation time series for U.S. climate divisions. J. Appl. Meteor. Climatol., **53**, 1232–1251, doi:10.1175/JAMC-D-13-0248.1.
65. Walsh, J., and Coauthors, 2014: Ch. 2: Our Changing Climate. Climate Change Impacts in the United States: The Third National Climate Assessment, J. M. Melillo, Terese (T.C.) Richmond, and G. W.

Yohe, Eds., U.S. Global Change Research Program, 19–67. doi:10.7930/J0KW5CXT.

66. Wang, R., J. Chen, X. Chen, and Y. Wang, 2017: Variability of precipitation extremes and dryness/wetness over the southeast coastal region of China, 1960–2014. Int. J. Climatol., doi:10.1002/joc.5113.
67. Westcott, N.E., Hollinger, S.E., and K.E. Kunkel, 2005: Use of real-time multisensor data to assess the relationship of normalized corn yield with monthly rainfall and heat stress across the central United States. J. Appl. Meteorol., **44**, 1667–1676, doi:10.1175/JAM2303.1.
68. Wilhite, D., 2006: Drought monitoring and early warning: Concepts, progress and future challenges. World Meteorological Organization. ISBN:978-92-63-11006-0.
69. Wuebbles, D., and Coauthors, 2014: CMIP5 Climate Model Analyses: Climate Extremes in the United States. Bull. Amer. Meteor. Soc., **95**, 571–583, doi:10.1175/BAMS-D-12-00172.1.
70. Xie, P., Chen, M., and W. Shi, 2010: CPC unified gauge-based analysis of global daily precipitation. *24th Conf. on Hydrology, Amer. Meteorol. Soc.*, Atlanta, Georgia, USA.
71. Xu, H., Chen, H., Wang, H., 2021. Future changes in precipitation extremes across China based onCMIP6 models. Int. J. Climatol., **42**, 635–651. doi:10.1002/joc.7264
72. Yazdanfar, Z., Sharma, A., 2015. Urban drainage system planning and design–challenges with climate change and urbanization: a review. Water Sci. Technol., **72**, 165–179. doi:10.2166/wst.2015.207
73. Yin, Y., and Coauthors, 2020: Cropland carbon uptake delayed and reduced by 2019 midwest floods. AGU Advances, doi:10.1029/2019AV000140.
74. Yoshimura, K., and M. Kanamitsu, 2008: Dynamical global downscaling of global reanalysis. Mon. Wea. Rev., **136**, 2983–2998, doi:10.1175/2008MWR2281.1.
75. Zhang, Q., Xu, C.-Y., Zhang, Z., 2009. Observed changes of drought/wetness episodes in the Pearl River basin, China, using the standardized precipitation index and aridity index. Theoretical and Applied Climatology, **98**, 89–99. doi:10.1007/s00704-008-0095-4
76. Zhang, W., T. Zhou, L. Zou, L. Zhang, and X. Chen, 2018: Reduced exposure to extreme precipitation from 0.5°C less warming in global land monsoon regions. Nat. Commun., **9**, 3153, doi:10.1038/s41467-018-05633-3.
77. Zhou, B., Xu, Y., Wu, J., Dong, S., Shi, Y., 2016. Changes in temperature and precipitation extreme indices over China: analysis of a high-resolution grid dataset. Int. J. Climatol., **36**, 1051–1066. doi:10.1002/joc.4400

Supplementary Files

Figures S1-S10 and Table S1 are not available with this version.

Figures

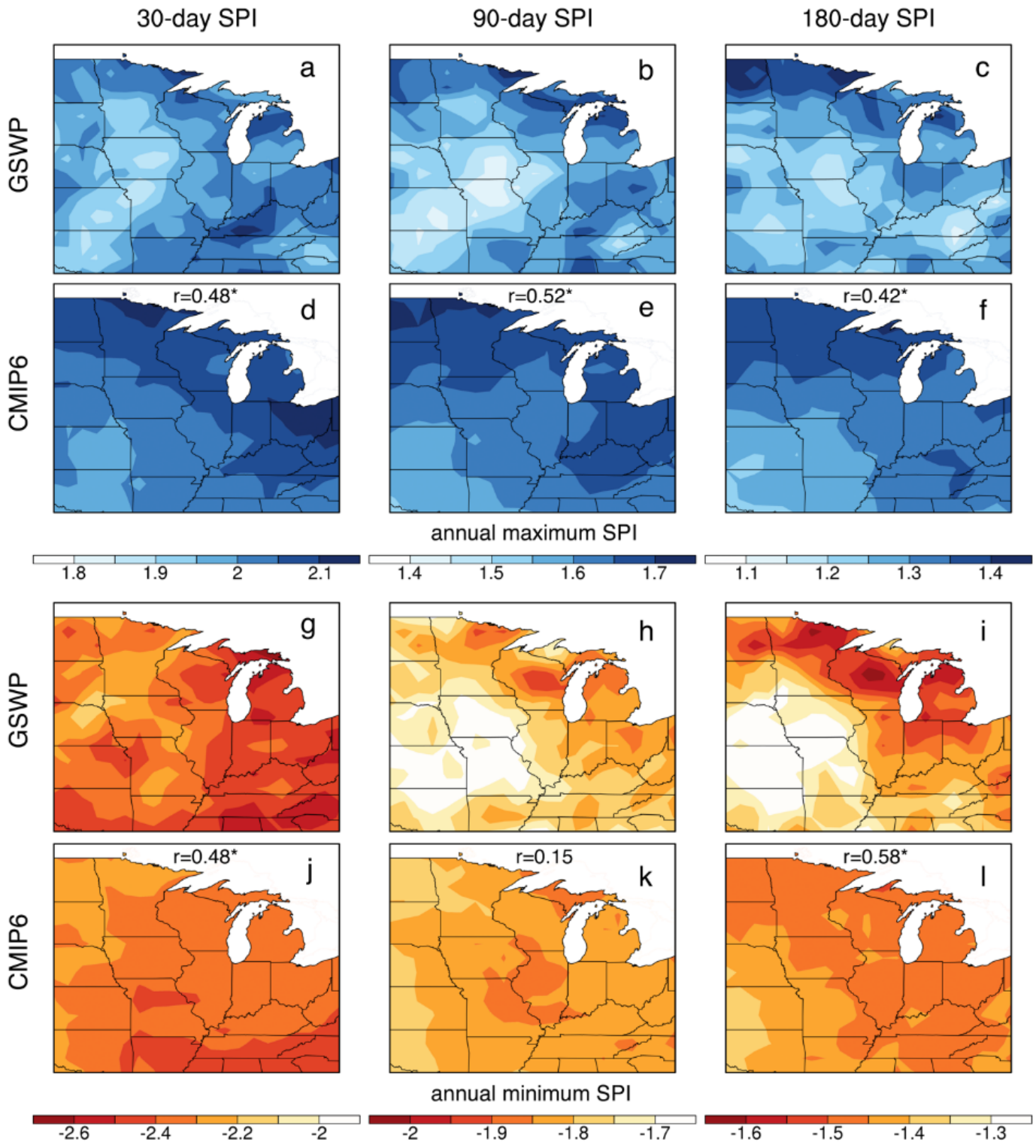

Figure 1

Climatology of annual maximum (a-f, unitless) and minimum (g-l, unitless) SPI during 1951-2014 based on 30-, 90-, and 180-day SPI in GSWP and CMIP6. Text in panels d-f and j-l shows the pattern correlation between CMIP6 and GWSP. An asterisk sign indicates the correlation is significant at the 95% confidence level.

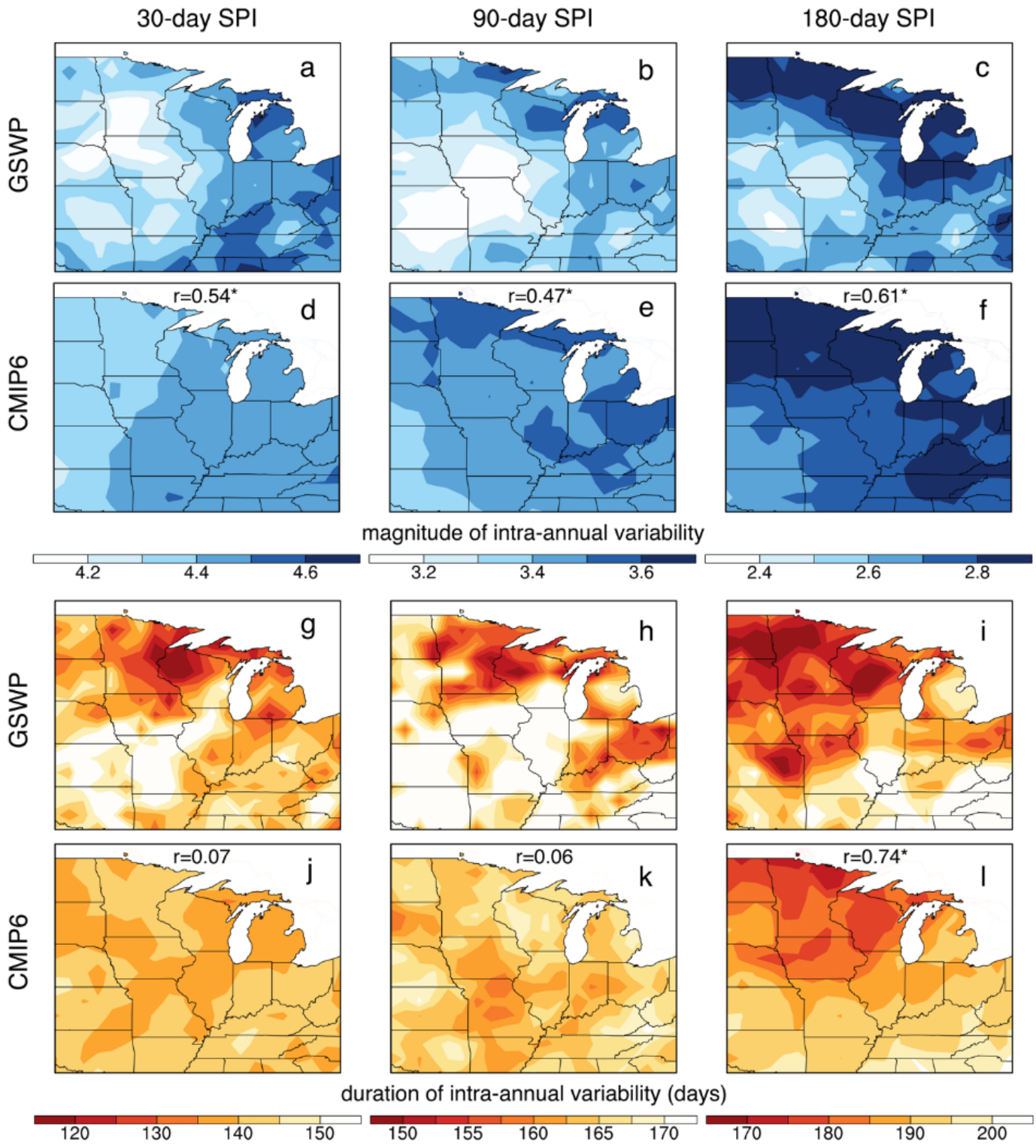

Figure 2

Climatology of the magnitude (a-f, unitless) and duration (g-l, in days) of intra-annual variability during 1951-2014 based on 30-, 90-, and 180-day SPI in GSWP and CMIP6. Text in panels d-f and j-l shows the pattern correlation between CMIP6 and GWSP. An asterisk sign indicates the correlation is significant at the 95% confidence level.

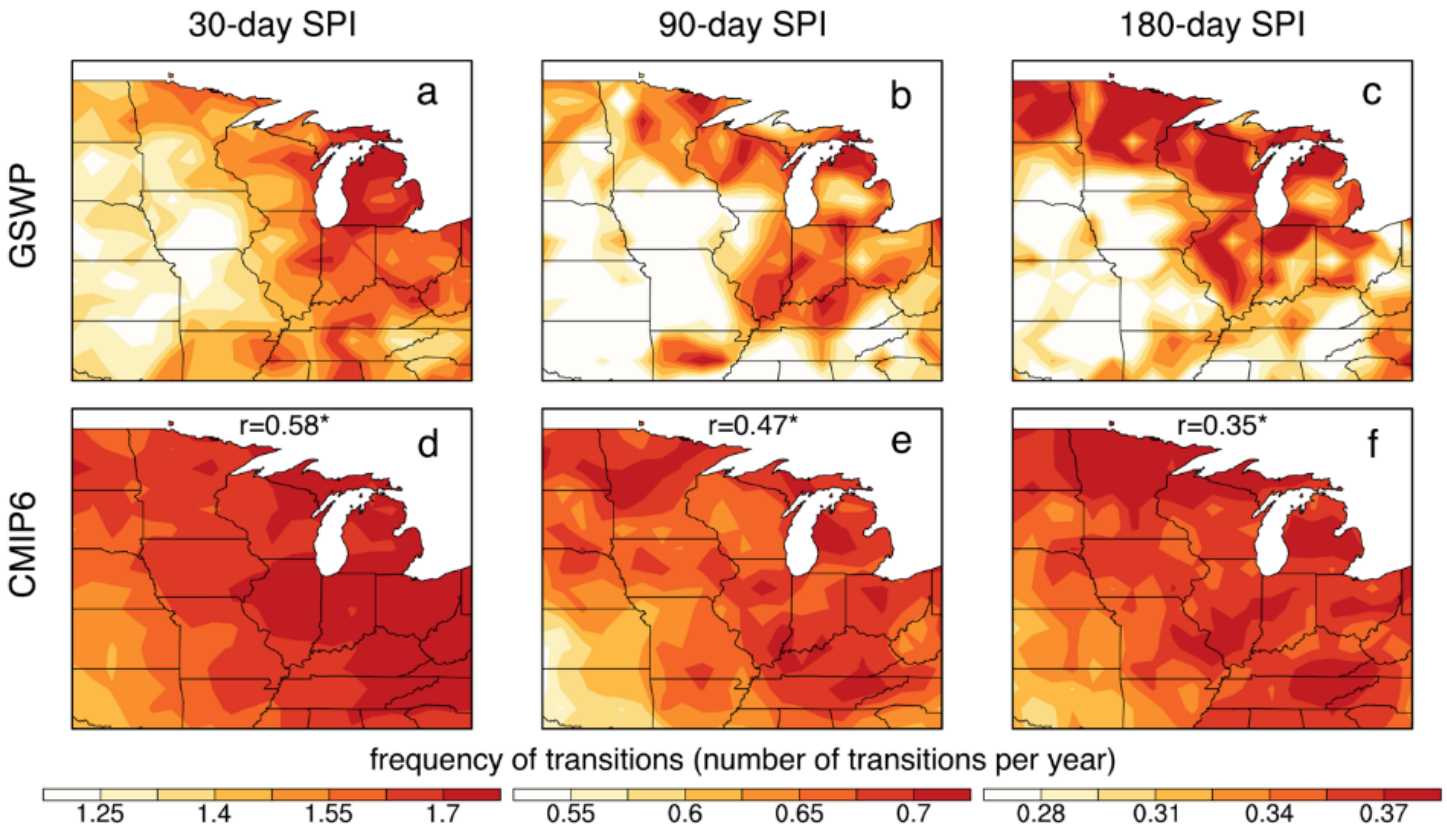

Figure 3

Frequency of precipitation extreme transitions (in number of transitions per year) during 1951-2014 based on 30-, 90-, and 180-day SPI in GSWP and CMIP6. Text in panels d-f shows the pattern correlation between CMIP6 and GWSP. An asterisk sign indicates the correlation is significant at the 95% confidence level.

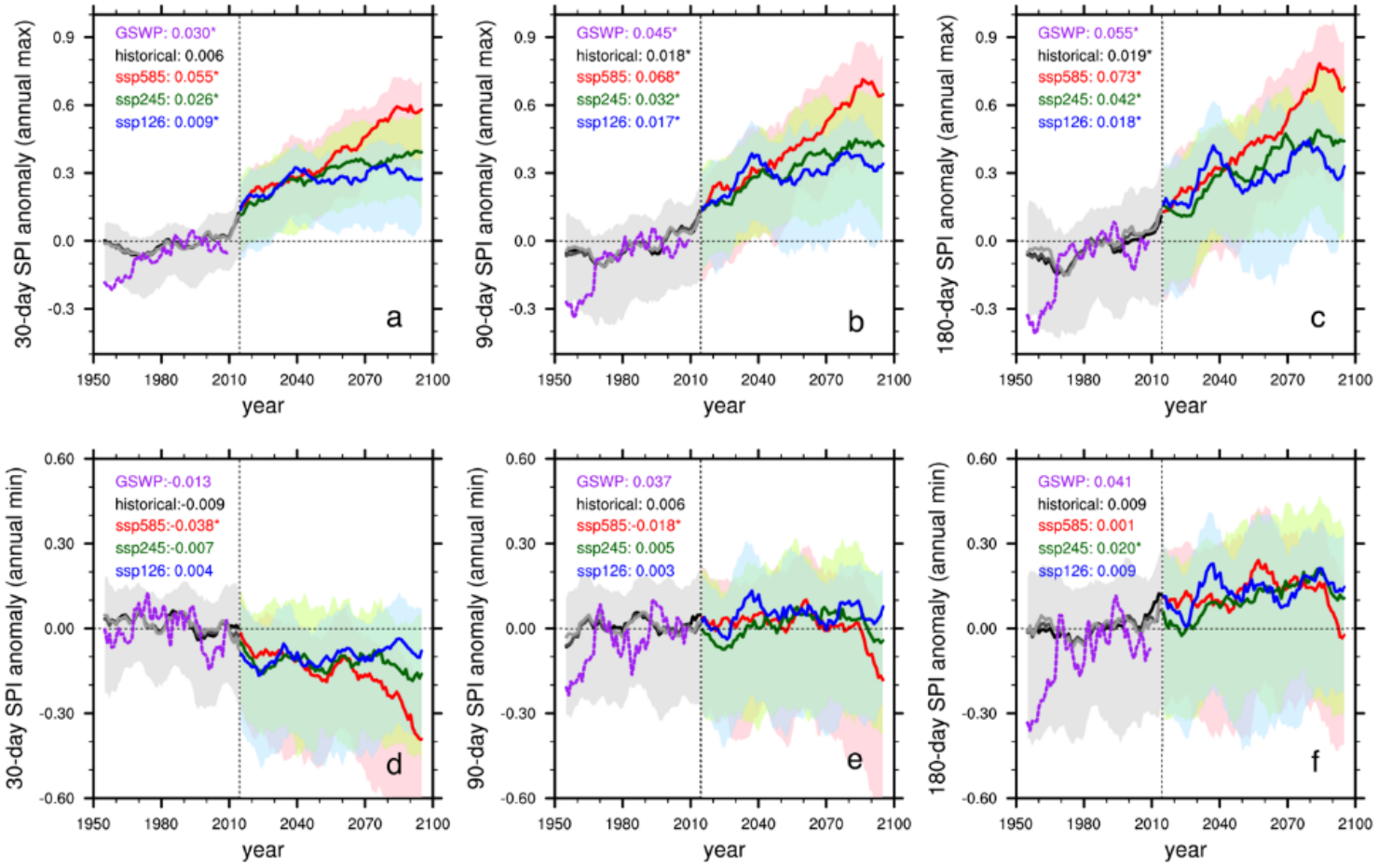

Figure 4

Time series of annual maximum (a-c, unitless) and minimum (d-f, unitless) SPI anomalies averaged across the Midwest during 1951-2100 based on 30-, 90-, and 180-day SPI. Anomalies are calculated based on the reference period 1981–2010. Shading shows the inter-model spread (25th and 75th percentiles). Time series are smoothed with a 10-year running average. Text in each panel shows the linear trend (in per decade) of annual maximum or minimum SPI. An asterisk sign indicates the trend is significant based on the Mann-Kendall non-parametric test. Colors of the text correspond to different datasets or different simulations. It should be noted that the thick black/gray lines for CMIP6 historical are based on three different sets of models that are available for SSP585, SSP245, and SSP126 (shown in Table 1), and they show consistency. The historical trend is calculated based on all available models.

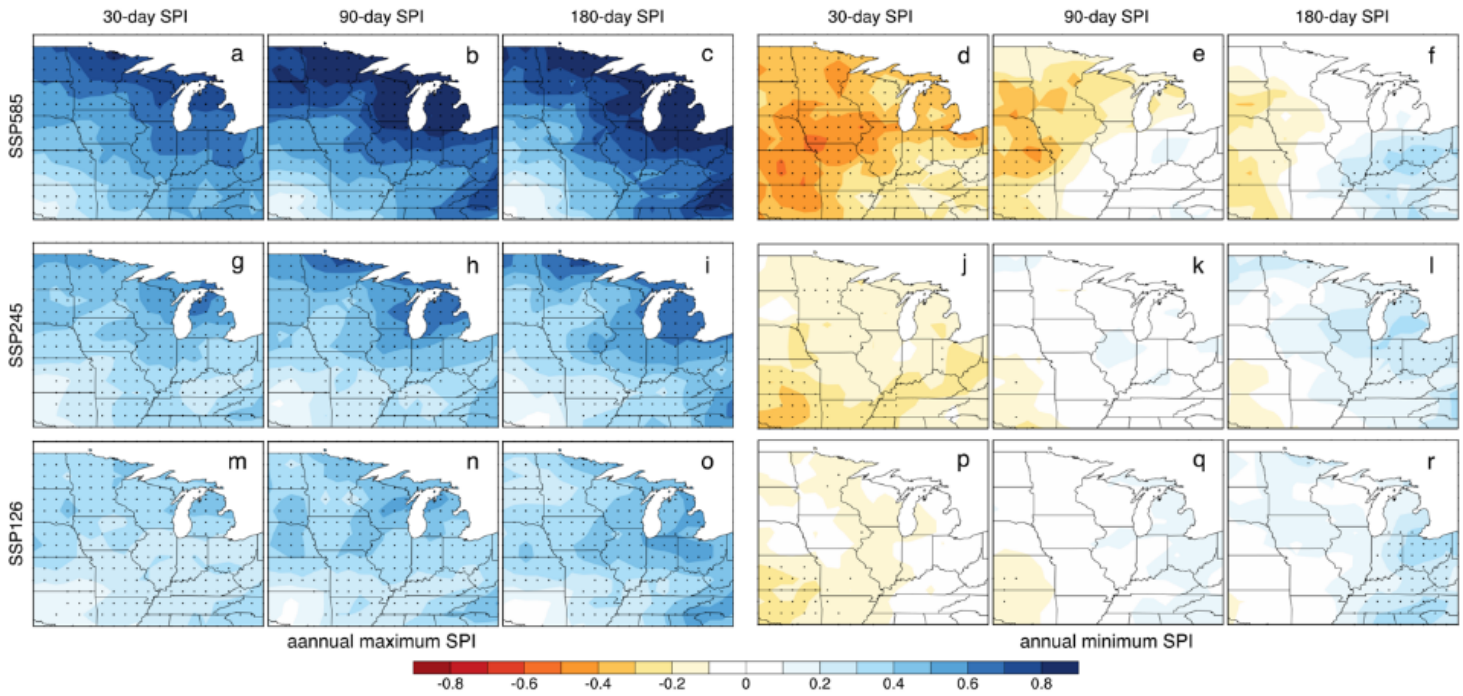

Figure 5

Projected changes in annual maximum and minimum SPI (unitless) over the time period 2071–2100 relative to the historical period 1981-2010 under the SSP585 (a-f), SSP245 (g-l), and sSP126 (m-r) scenarios. Stippling indicates the changes are statistically significant.

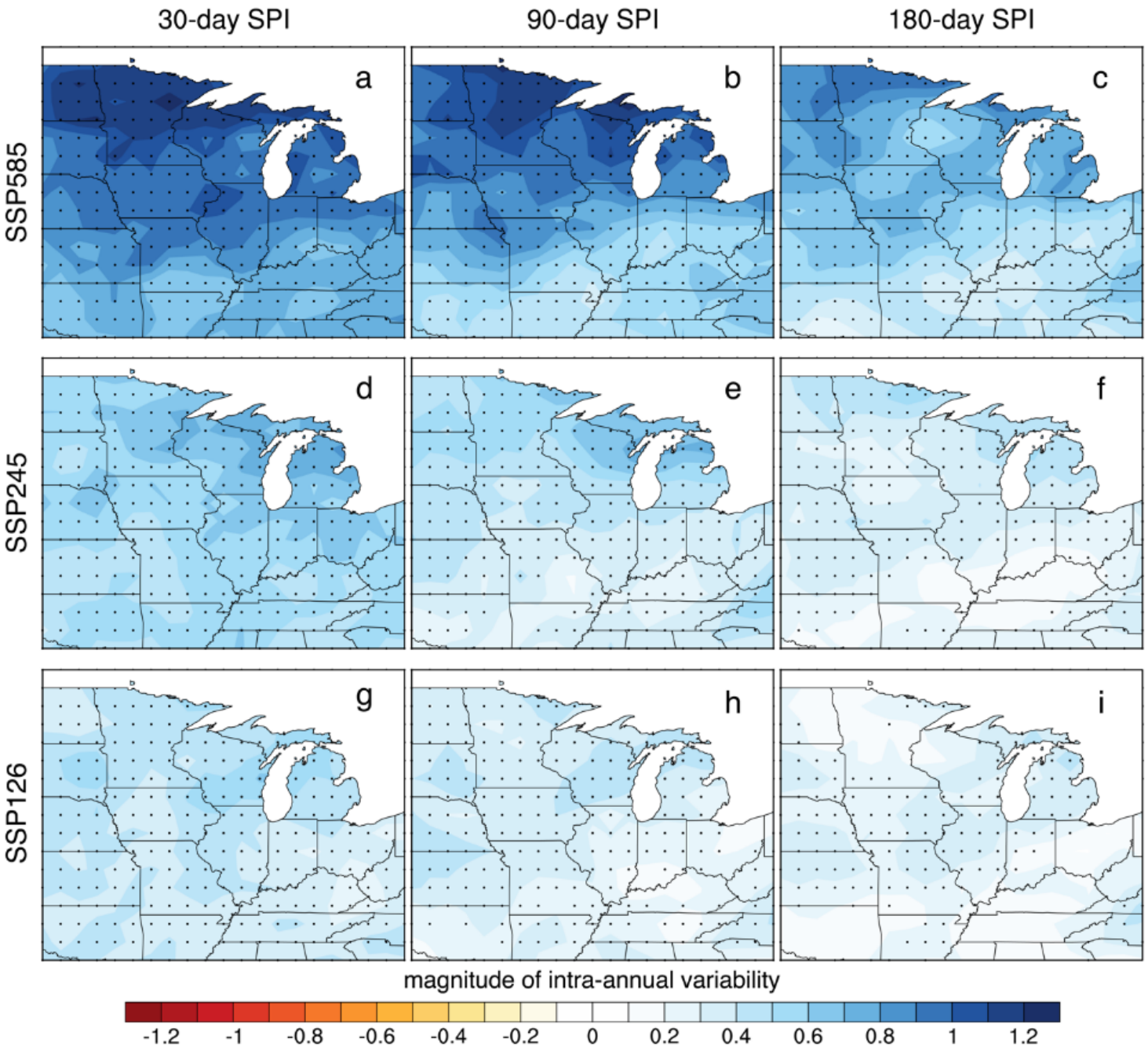

Figure 6

Projected changes in magnitude of intra-annual variability (unitless) over the time period 2071–2100 relative to the historical period 1981-2010 under the SSP585 (a-c), SSP245 (d-f), and sSP126 (g-i) scenarios. Stippling indicates the changes are statistically significant.

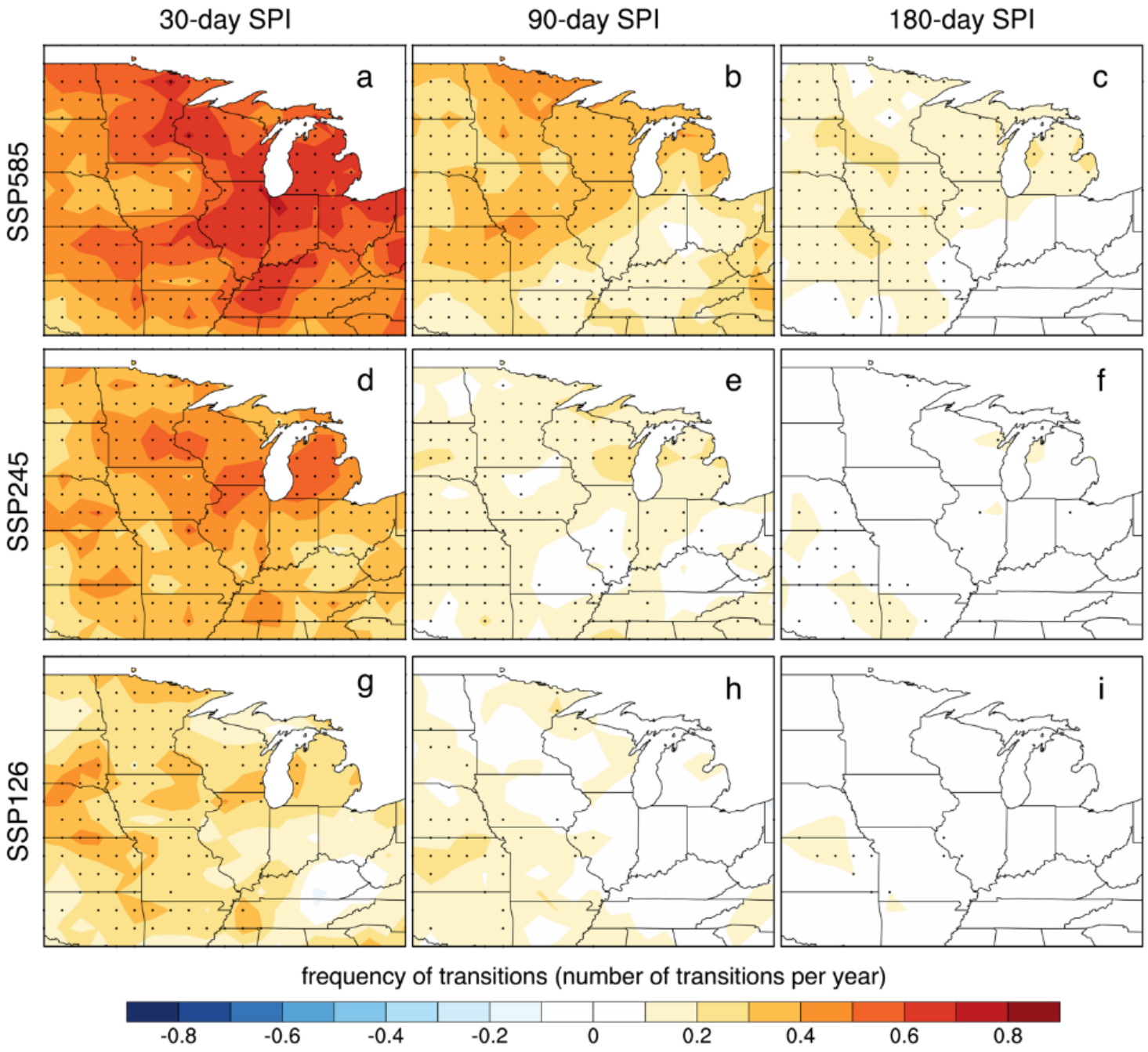

Figure 7

Projected changes in frequency of transitions (in number of transitions per year) over the time period 2071–2100 relative to the historical period 1981-2010 under the SSP585 (a-c), SSP245 (d-f), and sSP126 (g-i) scenarios. Stippling indicates the changes are statistically significant.

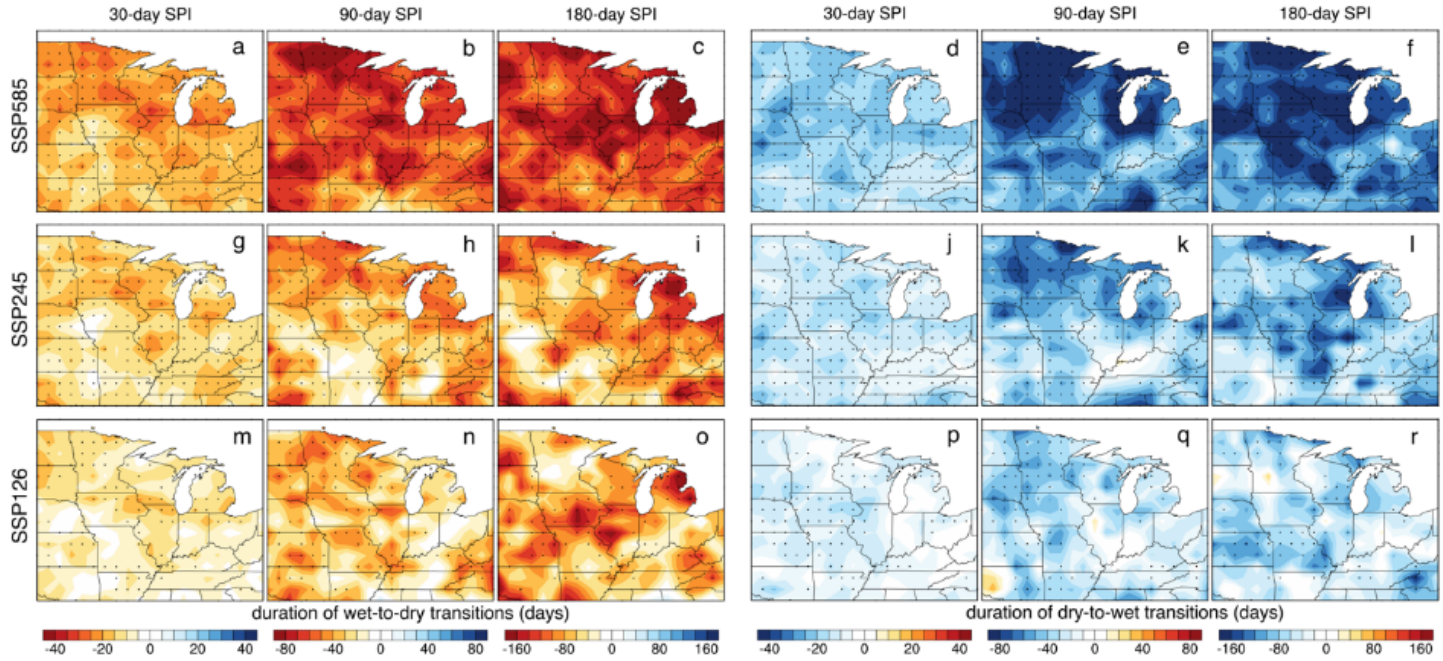

Figure 8

Projected changes in duration of transitions (in days) over the time period 2071–2100 relative to the historical period 1981-2010 under the SSP585 (a-f), SSP245 (g-j), and sSP126 (m-r) scenarios. Panels on the left are for the wet-to-dry transitions, and panels on the right are for the dry-to-wet transitions. Stippling indicates the changes are statistically significant.

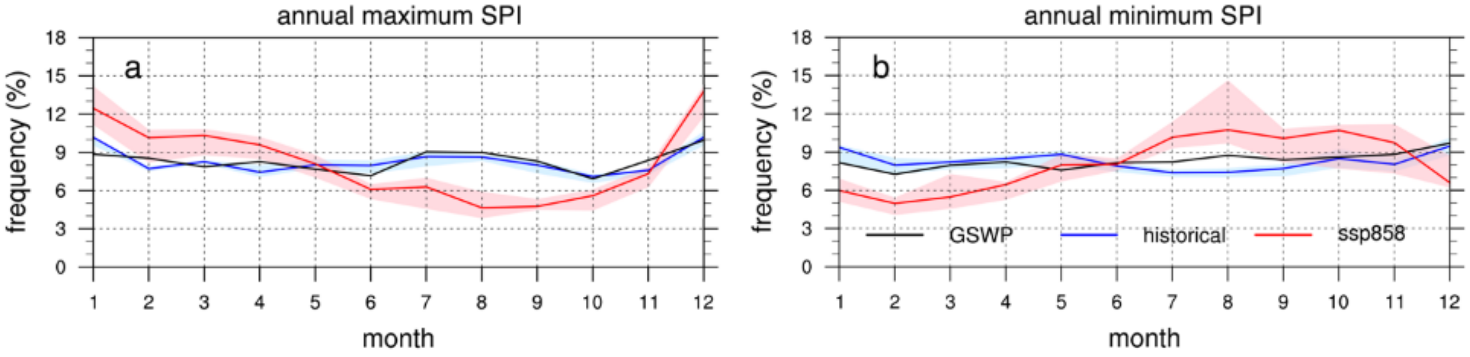

Figure 9

Frequency (in %) of the occurrence of maximum and minimum 30-day SPI in each month. The black and blue lines are GSWP and CMIP6 historical, respectively, for the period 1981-2010; the red line is CMIP6 SSP585 for the period 2071-2100. Shading shows the inter-model spread (25th and 75th percentiles).

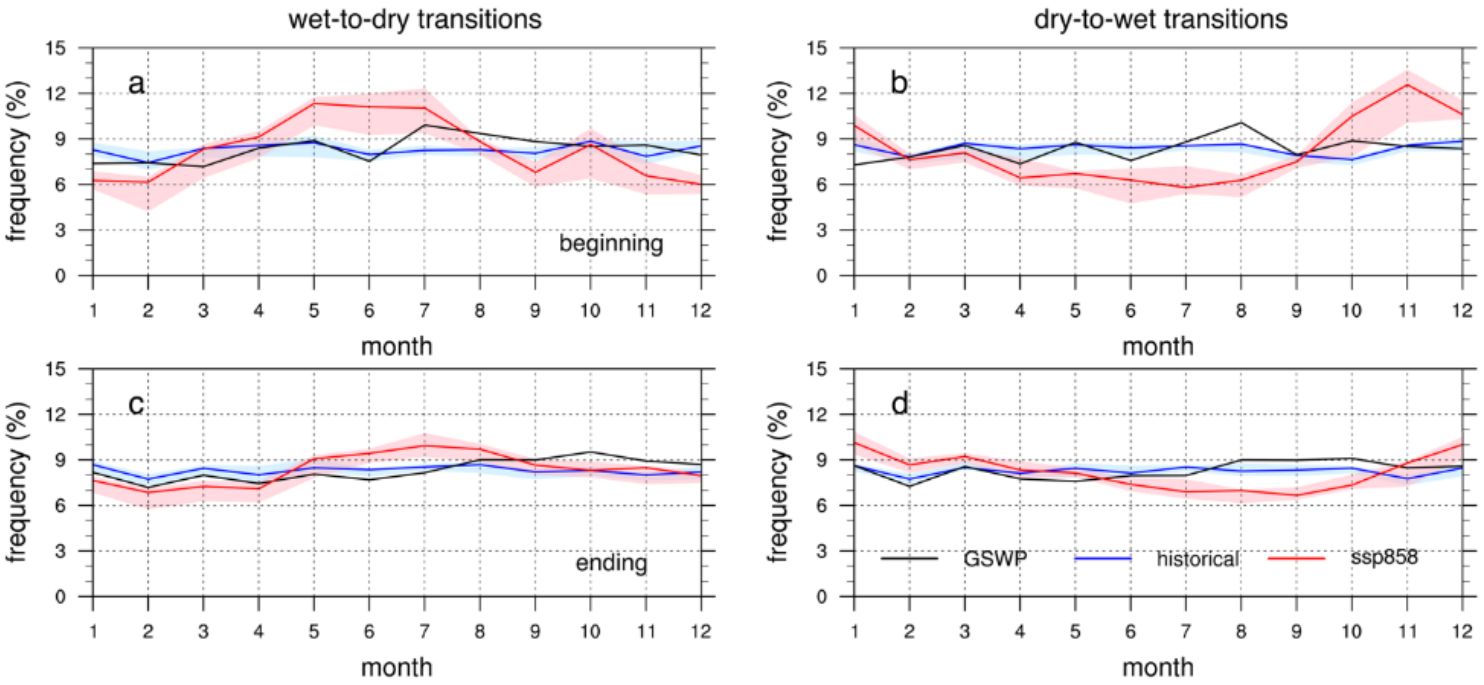

Figure 10

Frequency (in %) of the occurrence of wet-to-dry (a,c) and dry-to-wet (b,d) transitions in each month based on the 30-day SPI. Panels a,b show when the transition starts; panels c,d show when the transition ends. The black and blue lines are GSWP and CMIP6 historical, respectively, for the period 1981-2010; the red line is CMIP6 SSP585 for the period 2071-2100. Shading shows the inter-model spread (25th and 75th percentiles).